HAUPTMAN, H. A. (1972). *Crystal Structure Determination. The Role of the Cosine Seminvariants.* New York: Plenum.
HAUPTMAN, H. & GREEN, E. A. (1976). *Acta Cryst.* A**32**, 45-49.
RIGAMONTI, R. (1936). *Gazz. Chim. Ital.* **66**, 174-182.
SUTTON, L. E. (1958). Editor. *Tables of Interatomic Distances and Configuration in Molecules and Ions.* Spec. Publ. no. 11, p. 512. London: The Chemical Society.
TURNER, J. N., BARNARD, D. P., MCCAULEY, P. & TIVOL, W. F. (1991). In *Electron Crystallography of Organic Crystals,* edited by J. R. FRYER & D. L. DORSET, pp. 55-62. Dordrecht: Kluwer Academic Publishers.
UYEDA, N., KOBAYASHI, T., ISHIZUKA, K. & FUJIYOSHI, Y. (1978-1979). *Chem. Scr.* **14**, 47-61.
UYEDA, N., KOBAYASHI, T., SUITO, E., HARADA, Y. & WATANABE, M. (1972). *J. Appl. Phys.* **43**, 5181-5189.
VAINSHTEIN, B. K. (1964). *Structure Analysis by Electron Diffraction.* Oxford: Pergamon.
YAO, J. (1981). *Acta Cryst.* A**37**, 642-644.

Acta Cryst. (1992). A**48**, 568-574

Direct Methods in Electron Crystallography – Structure Analysis of Boric Acid

BY DOUGLAS L. DORSET

Electron Diffraction Department, Medical Foundation of Buffalo, Inc., 73 High Street, Buffalo, NY 14203, USA

(*Received* 11 *June* 1991; *accepted* 19 *February* 1992)

Abstract

Direct phasing methods based on the probabilistic estimate of triplet and quartet structure invariants are used to determine the crystal structure of boric acid from room-temperature electron diffraction data published by Cowley [*Acta Cryst.* (1953), **6**, 522-529] and also new low-temperature data collected at or below 128 K. In either instance, the resulting structure is the monolayer found earlier and the bond distances and angles for heavy atoms computed from the atomic coordinates agree well with three-dimensional X-ray and neutron diffraction determinations. H-atom positions are not accurately defined, however. A reason for the monolayer structure resulting from the analysis of electron diffraction data is suggested, given the continuous reciprocal-lattice rods observed in diffraction patterns from tilted crystals also seen earlier at room temperature.

Introduction

In the 1950s the utility of electron diffraction intensity data for crystal structure analysis was anticipated with considerable enthusiasm, especially for the materials where the favorable scattering-factor ratio would permit a more accurate determination of H-atom positions than is possible by X-ray crystallography (Cowley, 1953*a*). A number of structures were determined (Cowley, 1953*b*; Vainshtein, 1964) from such data but, due to the difficulties experienced in finding phases for the measured structure-factor amplitudes, contemporary X-ray structures were used to define the heavy-atom positions and the H-atom positions were then sought in the subsequent electrostatic potential maps. Unfortunately, this reasonable procedure has often created an unfavorable impression of the electron diffraction technique in the crystallographic community, an impression that is amplified by the relative complexity of the scattering theory and, thus, the number of corrections that sometimes need to be made to the measured data. That is to say, it is commonly thought by many crystallographers that valid *ab initio* structure analyses with electron diffraction intensity data are not possible.

Recently, this laboratory has investigated the use of direct phasing techniques for determining crystal structures from observed electron diffraction intensities, including a reassessment of data sets that were used in the earlier analyses. As has been shown (Dorset, 1991*a*), direct phase analysis of published electron diffraction data from 2,5-diketopiperazine (2,5-piperazinedione) (Vainshtein, 1955) yields a structure that is very close to the one found by an X-ray determination. Similar results were obtained (Dorset, 1991*b*) in the reanalysis of urea (Lobachev & Vainshtein, 1961) and thiourea (Dvoryankin & Vainshtein, 1960), although some influence of dynamical scattering was indicated in the latter case. Nevertheless, direct phasing methods, based on the evaluation of three- and four-phase invariants, are found to be remarkably robust when used with electron diffraction intensity data, even when they are somewhat perturbed by multiple scattering.

Among the earliest studies of hydrogen-bonded structures by electron diffraction, boric acid was found (Cowley, 1953*b*) to have a disordered layer stacking and the hydrogen-bonding scheme was quite different from the one suggested originally by Zachariasen (1934), since the possibility of nonlinear linkages is suggested in the final potential maps. This structure has not been verified in subsequent X-ray (Zachariasen, 1954; Gajhede, Larsen & Rettrup,

0108-7673/92/040568-07$06.00

1986) and neutron (Craven & Sabine, 1966) diffraction analyses. Since the electron diffraction data had been assigned phase values from the earliest X-ray structure, it is of particular interest to determine what results will be found from an *ab initio* structure analysis in which no *a priori* assumptions are made about the heavy-atom positions. The results of this direct phase determination are described below.

Data and methods

One single-crystal electron diffraction intensity data set used for the structure analysis was originally published by Cowley (1953*b*) and was collected at room temperature. In all of the analyses presented here, which use Cowley's uncorrected data, it is assumed that the 133 measured quantities are sufficiently close to their kinematical values to permit an *ab initio* structure determination. The space group assumed by Cowley (1953*b*) is $P\bar{1}$ and the unit-cell dimensions originally given by Zachariasen (1934) were used, *i.e.*

$$a = b = 7.04(4),\ c = 6.56\ (4)\ \text{Å},$$
$$\alpha = 92.5,\ \beta = 101.2,\ \gamma = 120.0°.$$

Note that a hexagonal layer packing is implied by these parameters. Although these dimensions are retained for this study, subsequent determinations (Zachariasen, 1954; Craven & Sabine, 1966) have shown that the hexagonal symmetry is not actually present. Nevertheless, the deviation from this is 0.016 Å in the a-axis length and only 0.17° in the γ angle. Such precision is near the limits of selected-area electron diffraction measurements.

Several other selected-area diffraction data sets were collected at low temperature and at 100 kV using a JEOL JEM-100CXII electron microscope equipped with a Gatan 626 low-temperature specimen holder for the goniometer stage and also a Gatan 651N low-temperature anticontamination device. Boric acid (ACS Grade, Fisher Scientific Co., Fair Lawn, NJ, USA) was crystallized by slow evaporation of a dilute aqueous solution onto carbon-film-covered 400-mesh copper electron-microscope grids and the presence of crystals was detected with a polarizing light microscope. In a typical experiment, liquid nitrogen was added to the standard anticontamination trap and then the Gatan anticontaminator, allowing the temperature of the latter to drop to 98K before the sample was inserted into the column. After the grid was injected into the sample holder in its capsule, the port to the isolation vessel was closed to prevent accumulation of additional humidity from the outside. A small amount of liquid nitrogen was introduced into the Dewar vessel to cool the tip below 273K. The holder was then inserted into the microscope vacuum. During the transfer, the presence of a sliding shield prevented ice buildup on the grid and, once the specimen holder tip was evacuated in the column, more liquid nitrogen was added to cool the specimen to 128 K before commencement of electron diffraction and bright-field-imaging experiments. During these experiments, the temperature would fall further, to, for example, 108 K. The rather complicated process prevented excessive contamination of the specimen with ice as evidenced by the electron diffraction patterns (Fig. 1). As usual, care was taken to minimize electron irradiation of the sample by control of illumination conditions and use of a sensitive photographic film (Kodak DEF5). The diffraction camera length was calibrated with an Au powder sample on the same specimen grid, preferably using diffraction films that included both the boric acid and gold patterns. From these measurements was obtained

$$a = b = 7.17\ (1)\ \text{Å},\ \gamma = 120.0°.$$

The 83 unique diffraction intensities (quantitatively measured by integration of peaks in film scenes with a Joyce Loebl MKIIIC flatbed microdensitometer) betrayed local violations of hexagonal symmetry, perhaps due to small irregular crystal bends (Fig. 1).

For the room-temperature data, the 133 unique intensities were used to calculate normalized structure factors,

$$|E_h|^2 = |F_h|^2 / \sum_i f_i^2,$$

where $|F_h|$ are observed structure-factor magnitudes and f_i are Doyle–Turner electron scattering factors (Doyle & Turner, 1968). A Wilson (1942) plot of the

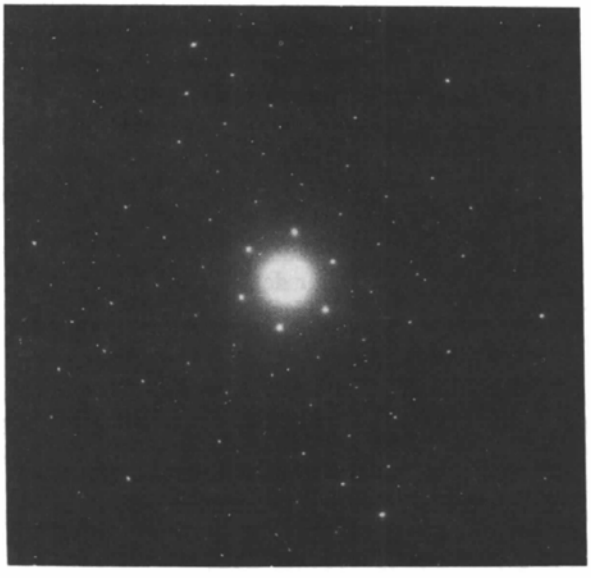

Fig. 1. Electron diffraction pattern from boric acid observed at $T \leq 128$ K.

Table 1. *Distribution of $|E_h|$ values for boric acid*

	Theoretical		
	Centrosymmetric	Non-centrosymmetric	Experimental
$\langle\|E^2\|\rangle$	1.000	1.000	1.00
$\langle\|E^2-1\|\rangle$	0.968	0.736	0.71
$\langle\|E\|\rangle$	0.798	0.886	0.89
$\%\|E\|>3.0$	0.3	0.01	0.8
$\%\|E\|>2.0$	5.0	1.8	2.3
$\%\|E\|>1.0$	32.0	37.0	24.8

observed data indicated that the overall isotropic temperature factor was $B = 0.0$ Å^2. Therefore, no temperature factor was used for the calculation of $|E_h|$. The distribution of $|E_h|$ for this data set is shown in Table 1. Upon comparison with expected values for centrosymmetric or noncentrosymmetric structures (Karle, Dragonette & Brenner, 1965), the distribution is shown not to conform to space group $P\bar{1}$. (This is probably because the intensity set is too small a sample of the whole reciprocal lattice.)

Similar calculations of normalized structure factors were made for four separate low-temperature data sets, also regarding them initially to be triclinic structures, although some data sets were later averaged to correspond to hexagonal symmetry.

Direct phase determination was based on the probabilistic estimate of $\sum_2$-triple (as well as a few $\sum_1$-triple) invariants (Hauptman & Karle, 1953; Hauptman, 1972) as well as quartet invariants (Hauptman & Green, 1976), again in space group $P\bar{1}$. In the latter case, we exploited the use of 'cross-term' magnitudes for the estimate of 0, π quartet phases (Hauptman, 1975) as described in our original application to electron diffraction data (Dorset & Hauptman, 1976). Application of these procedures to electron diffraction data sets has been discussed further in more recent papers (Dorset, 1991*a*, *b*).

Results

For the room-temperature data, 86 reflections with $|E_h| \geq 0.70$ were used to generate three- and four-phase structure invariants. Of these, four positive and one negative $\sum_1$-triples were accepted. Additionally, 16 $\sum_2$-triples, where $A \geq 3.85$, and 35 quartets, where $B \geq 12.0$, were used. After defining the origin by setting $\varphi_{\bar{6}30} = 0$, $\varphi_{\bar{3}60} = 0$, phase relationships among 28 reflections could be defined if two symbols for phase values were included, thus requiring the calculation of four potential maps. The sequence of the phase determination for this data set is outlined in Table 2. The potential map selected for the structure determination is shown in Fig. 2(*a*) and its choice is based on a possible threefold geometry of the borate group which could be linked in a pseudo-hexagonal array by hydrogen bonds. However, there is another peak in this map (arrowed) which is spurious and was not used for the initial structure-factor calculation.

Table 2. *Sequence of phase determination for room-temperature electron diffraction data from boric acid*

Origin definition: $\varphi_{\bar{6}30} = \varphi_{\bar{3}60} = 0$
$\sum_1$-triples: $\varphi_{\bar{8}20} = \varphi_{620} = \varphi_{260} = \varphi_{\bar{6}80} = 0$, $\varphi_{460} = \pi$
$\sum_2$-triples: $\varphi_{330} = 0$; $\varphi_{900} = 0$; $\varphi_{\bar{9}90} = 0$; $\varphi_{090} = 0$
Let $\varphi_{\bar{1}10} = a \rightarrow \sum_2$-triple: $\varphi_{\bar{5}20} = a$
Let $\varphi_{\bar{1}40} = b \rightarrow \sum_2$-triples: $\varphi_{\bar{4}10} = b$, $\varphi_{510} = b$, $\varphi_{\bar{7}40} = a$
$\varphi_{150} = b$, $\varphi_{130} = \pi$, $\varphi_{\bar{2}50} = a$
$\varphi_{\bar{4}30} = \pi$, $\varphi_{\bar{5}60} = \pi$, $\varphi_{700} = \pi$
Positive quartets: $\varphi_{\bar{2}90} = \pi$, $\varphi_{200} = \pi$, $\varphi_{420} = \pi$, $\varphi_{\bar{2}20} = b$, $\varphi_{\bar{1}60} = \pi$
Correct map calculated when $a = b = \pi$

When the threefold borate geometry found in this initial map is used to calculate structure factors the crystallographic residual to the total observed data set is 0.39. The total phase set is then used to calculate a second potential map (Fig. 2*b*), which clearly reveals the arrangement of the heavy-atom positions and supports the choice of quasi-hexagonal positions proposed originally by Cowley (1953*b*). If these new heavy-atom positions are used to calculate structure factors, the R factor drops to 0.29. (There are only seven phases that disagree with the values listed earlier.) H-atom positions are found by computation of a Fourier map based on $2|F_o| - |F_c|$, but their locations are not well defined (Fig. 2*c*). They can also be seen if only reflections where $|E_h| \geq 0.85$ are used to calculate the potential map (Fig. 2*d*). In addition to sites that would hydrogen bond opposing O atoms in facing borate trimers, density can also be found around the center of symmetry relating these two groups. If six unique H-atom positions are assigned in this way with half occupancy, the R factor is 0.27. If, on the other hand, only three H-atom positions are used that correspond, more or less, to the hydrogen-bonding scheme determined by X-ray and neutron diffraction analyses, the R factor is again 0.29. Final bond distances and angles obtained from the room-temperature analysis can be compared to the values given by Craven & Sabine (1966): ⟨B-O⟩: 1.36 (1) Å (1.367 Å); ⟨O-B-O⟩: 120.1 (2)° (120°); ⟨O-H⟩: 1.11 (11) Å (0.97 Å); ⟨B-O-H⟩: 111.3 (60)° (113.3°).

Phase determination for the low-temperature data sets is very similar to the process described above. Again, symbolic phase values are needed to solve the structure, requiring calculation of eight potential maps. After the heavy-atom positions are assigned, even when only triclinic symmetry is assumed in the diffraction intensity distribution, the single-layer array similar to Fig. 2(*b*) is found and all attempts to locate a second layer or fractional occupancies of this second layer lead to failure.

A structure solution for a data set that had been symmetrized to correspond to a hexagonal packing is illustrated in Fig. 3. After direct phasing (where assumption of hexagonal symmetry allows one to reduce three symbolic phases to one), the initial potential map based on 23 unique reflections contains

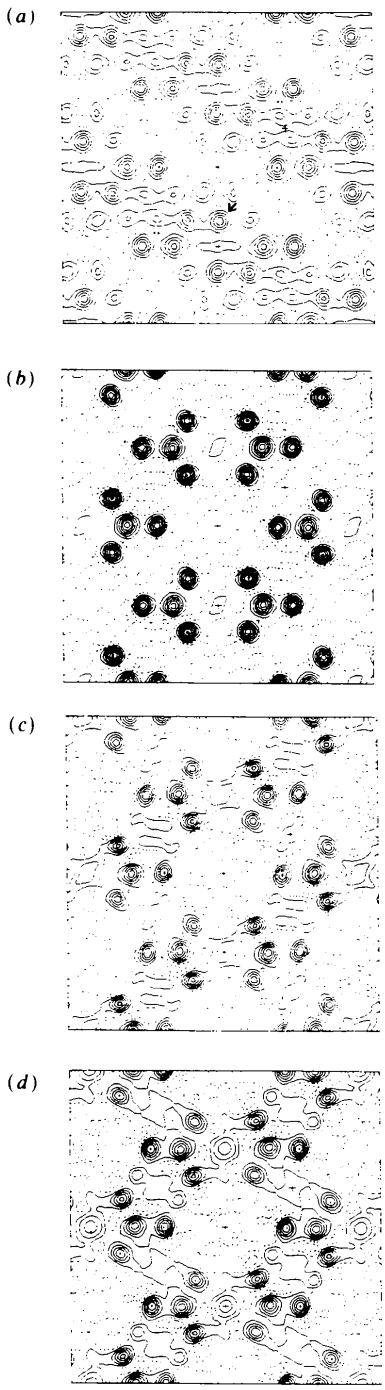

Fig. 2. Analysis of room-temperature data of Cowley (1953*b*). (*a*) Initial potential map based on 28 reflections correctly phased by direct methods and choice of algebraic unknowns $a = \pi$, $b = \pi$. (*b*) Potential map calculated using $|F_o|$ from all 133 measured reflections phased from the heavy-atom sites chosen from (*a*). The new heavy-atom sites lie on the pseudohexagonal positions chosen by Cowley (1953*b*) even though only $P\bar{1}$ symmetry is assumed. (*c*) Difference map based on $2|F_o| - |F_c|$. Several possible positions for H atoms are suggested. (*d*) Potential map calculated with reflections where $|E_h| \geq 0.85$. H-atom positions are again visible.

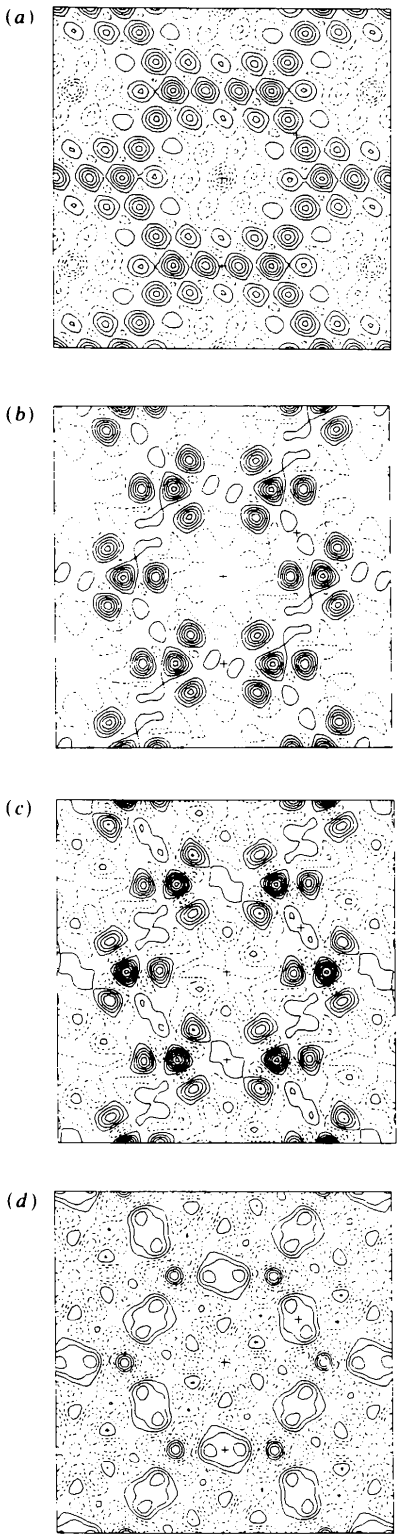

Fig. 3. Analysis of low-temperature electron diffraction data. (*a*) Initial potential map based on 23 reflections phased *via* triplet and quartet invariants. (*b*) Initial map calculated from complete phase set (83 reflections) after heavy-atom positions are located in (*a*); (*c*) $2|F_o| - |F_c|$ map; (*d*) $|F_o| - |F_c|$ map.

more spurious peaks than found before (Fig. 3*a*). This may be partially due to the (slightly) lower resolution of the initially phased reflections compared to the analysis of the room-temperature data. Assignment of heavy-atom positions again produces a map from the total set of 83 phased structure factors, which does not suggest a second layer (Fig. 3*b*). From the initial estimate of heavy-atom positions, the R factor is 0.35 and if Cowley's six H-atom positions are included this value drops to 0.31. Next, positions of the heavy atoms were then averaged to correspond to the assumed hexagonal symmetry (since only $P\bar{1}$ symmetry was used for the structure-factor calculation). An attempt was then made to find H atoms in a $2|F_o|-|F_c|$ map (Fig. 3*c*), but, even though the R factor is lowered, the resulting O–H bond lengths are much too long. Next, an $|F_o|-|F_c|$ synthesis was used (Fig. 3*d*) and the H-atom positions were constrained to circles radiating from the center of the O atoms and directed to touch the highest-density regions of the difference map. When their positions are symmetrized and the temperature factors are adjusted so that $B_B = 1.0$, $B_O = 2.0$, $B_H = 3.0$ Å^2, the final R factor is 0.30. (With another independent symmetrized data set corresponding to the pattern in Fig. 1, $R = 0.29$ for 86 independent reflections. These values are listed in Table 3.) The final coordinates (given in Table 4) may be used to obtain the values

$$\langle d_{B\text{-}O}\rangle = 1.33\ (1)\ \text{Å}$$
$$\langle d_{O\text{-}H}\rangle = 1.07\ (1)\ \text{Å}$$
$$\langle \text{O-B-O}\rangle = 120.0\ (11)^\circ$$
$$\langle \text{B-O-H}\rangle = 93.4\ (8)^\circ.$$

Note that the B–O–H angle is somewhat small, owing to the fact that the H-atom positions do not correspond closely to the values found in X-ray or neutron diffraction determinations (Table 4).

Table 3. *Observed and calculated structure factors for boric acid (low temperature)*

hk	$\lvert F_o\rvert$	F_c	hk	$\lvert F_o\rvert$	F_c
10	1.61	−1.73	$\bar{4}3$	0.94	−0.98
20	0.77	−1.26	$\bar{5}3$	0.65	−0.13
30	0.40	−0.41	$\bar{6}3$	1.51	1.28
40	0.69	0.81	$\bar{7}3$	0.47	−0.27
50	0.56	0.38	04	0.69	0.81
60	0.37	−0.27	14	0.57	0.44
70	0.35	−0.36	24	0.52	−0.40
01	1.61	−1.73	34	0.47	−0.28
11	0.75	1.10	$\bar{1}4$	0.94	−0.91
21	0.80	0.73	$\bar{2}4$	0.66	0.28
31	0.94	−0.93	$\bar{3}4$	0.92	−1.13
41	0.52	0.24	$\bar{4}4$	0.69	0.83
51	0.57	−0.46	$\bar{5}4$	0.52	0.25
61	0.42	0.47	$\bar{6}4$	0.49	−0.40
$\bar{1}1$	1.61	−1.74	$\bar{7}4$	0.45	−0.37
$\bar{2}1$	0.75	1.10	05	0.56	0.38
$\bar{3}1$	0.73	1.20	15	0.57	−0.43
$\bar{4}1$	0.92	−1.06	25	0.35	0.21
$\bar{5}1$	0.57	0.43	35	0.35	−0.28
$\bar{6}1$	0.57	−0.43	$\bar{1}5$	0.52	0.24
$\bar{7}1$	0.37	0.42	$\bar{2}5$	0.65	−0.11
02	0.77	−1.26	$\bar{3}5$	0.85	−0.42
12	0.73	1.22	$\bar{4}5$	0.57	0.44
22	0.66	0.28	$\bar{5}5$	0.56	0.35
32	0.65	−0.12	$\bar{6}5$	0.52	−0.43
42	0.49	−0.42	$\bar{7}5$	0.41	0.27
52	0.53	0.28	06	0.37	−0.27
62	0.42	0.16	16	0.37	0.41
$\bar{1}2$	0.75	1.10	$\bar{1}6$	0.57	−0.47
$\bar{2}2$	0.77	−1.31	$\bar{2}6$	0.49	−0.43
$\bar{3}2$	0.80	0.75	$\bar{3}6$	1.51	1.28
$\bar{4}2$	0.66	0.28	$\bar{4}6$	0.52	−0.38
$\bar{5}2$	0.86	−0.39	$\bar{5}6$	0.57	−0.39
$\bar{6}2$	0.52	−0.41	$\bar{6}6$	0.37	−0.32
$\bar{7}1$	0.35	0.21	$\bar{7}6$	0.44	0.46
03	0.40	−0.41	07	0.35	−0.36
13	0.92	−1.07	$\bar{1}7$	0.42	0.47
23	0.86	−0.40	$\bar{2}7$	0.53	0.28
33	1.51	1.28	$\bar{3}7$	0.45	−0.34
43	0.45	−0.35	$\bar{4}7$	0.47	−0.30
$\bar{1}3$	0.80	0.72	$\bar{5}7$	0.35	0.20
$\bar{2}3$	0.73	1.24	$\bar{6}7$	0.37	0.40
$\bar{3}3$	0.40	−0.33	$\bar{7}7$	0.35	−0.31

Discussion

From the above analysis, it is clear that the observed electron diffraction intensities from thin microcrystals of boric acid, at both ambient and low temperatures, represent the coherent scattering from an isolated layer and not the true unit-cell contents. In fact, if the total unit-cell coordinates determined by Zachariasen (1954) are used for a structure-factor calculation, then the match to the observed data at room temperature is $R = 0.48$. Although the notion of a strict hexagonal layer packing is rejected by those who have carried out three-dimensional determinations with data from larger crystals, a case can be made for such packing in the thinner crystals. For example, Zachariasen's (1954) atomic coordinates from a single boric acid layer, with the same thermal parameters used for our structure-factor calculations, produce a poorer fit to the electron diffraction data ($R = 0.40$) than the hexagonal structure suggested by Cowley (1953*b*). Although the third dimension was not sampled in the original electron diffraction structure analysis, except to show that the reciprocal-lattice rods in this direction are continuous, the disorder model proposed by Cowley assumes that the heavy-atom coordinates in a layer are coplanar. This also contradicts the results of the three-dimensional structure analyses, since a weak interplanar interaction has been described (Craven & Sabine, 1966). However, the observation of continuous reciprocal-lattice rods is significant. At low temperature, continuous tilts of the crystalline specimen at 5° intervals again reveal the earlier observation that there is no place at which a reciprocal-lattice rod reaches zero intensity, as shown in Fig. 4. On average, then, there is no coherent interference function between two adjacent layers, thus each hexagonal layer scatters incoherently from the next.

Table 4. *Final atomic positions for boric acid*

	This determination (low temperature)		Zachariasen (1954)*		Gajhede *et al.* (1986)*		Craven & Sabine (1966)*	
	x/a	*y/b*	*x/a*	*y/b*	*x/a*	*y/b*	*x/a*	*y/b*
B	0.666	0.334	0.670	0.333	0.673	0.332	0.670	0.332
O1	0.454	0.226	0.448	0.208	0.450	0.207	0.451	0.208
O2	0.774	0.226	0.792	0.234	0.796	0.232	0.795	0.232
O3	0.774	0.546	0.786	0.556	0.770	0.556	0.769	0.555
H1	0.443	0.371	0.371	0.267	0.385	0.299	0.372	0.291
H2	0.629	0.072	0.695	0.078	0.709	0.077	0.710	0.073
H3	0.928	0.557	0.914	0.615	0.925	0.626	0.922	0.627

*After origin shift (0.024, −0.094) for single layer.

Another possible way of accounting for the effective single-layer scattering would be to suppose that crystal bending is severe enough to result in the diffraction incoherence described by Cowley (1961) and used to explain the observed electron diffraction from, for example, layered silicate structures (Cowley & Goswami, 1961). This kinematical argument states that the elastic bend distortion affects the actual Patterson function of the crystal, hence

$$I(s) = \sum_i w_i(\mathbf{s}) \exp(2\pi i \mathbf{r}_i \cdot \mathbf{s}) \exp(-\pi^2 c^2 s^2 z_i^2), \quad (1)$$

where $w_i(\mathbf{s})$ is the scattering factor corresponding to the ith Patterson peak at position $\mathbf{r}_i$, c is the crystal

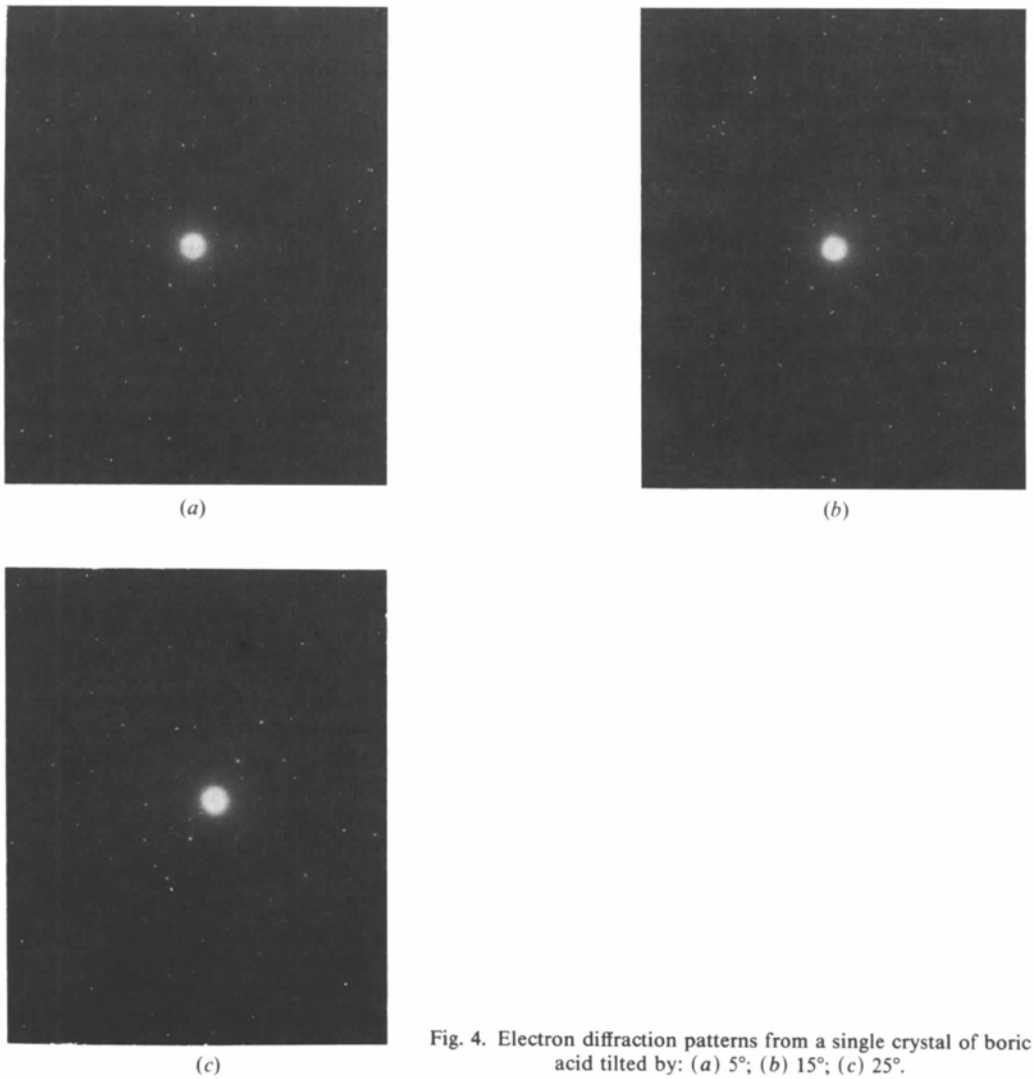

(*a*) (*b*) (*c*)

Fig. 4. Electron diffraction patterns from a single crystal of boric acid tilted by: (*a*) 5°; (*b*) 15°; (*c*) 25°.

bending in radians and z_i is the component of $\mathbf{r}_i$ in the electron-beam direction. If one starts with Zachariasen's (1954) bilayer crystal structure, a crystal-bend model can be shown (Fig. 5) to produce intensities that correspond less and less to the Fourier transform of the total unit-cell contents with increasing crystal bend, whereas they resemble more and more the scattering from a single layer. However, although indications of small bend distortion are found in the diffraction pattern (Fig. 1), bright-field images of the crystals do not contain sharp bend contours. Also, based on previous experience with epitaxially oriented crystals of small organic molecules (Dorset, 1989) and linear polymers (Moss & Dorset, 1982), a 6.56 Å unit-cell c spacing for boric acid should lie well within the coherent diffraction range, allowing visualization of the total unit-cell contents. If only single layers are scattering incoherently from one another, how does one account for the rather large R factor?

In such a situation, secondary scattering of the kind described by Cowley, Rees & Spink (1951) could be very important. If one regards the diffraction pattern in Fig. 1 to be from a centered orthorhombic structure where only $h+k=2n$ reflections are observed, then the convolution of intensities

$$\sum_{\mathbf{k}} I_{\mathbf{h}} I_{\mathbf{h}-\mathbf{k}} = I_{\mathbf{h}} * I_{\mathbf{h}}$$

will retain the $h+k=2n+1$ absences. However, this perturbation can have a sizeable effect on the observed intensities $I_{\mathbf{h}'}$ if $I_{\mathbf{h}'} = I_{\mathbf{h}} + mI_{\mathbf{h}} * I_{\mathbf{h}}$ and * represents the convolution operator. If the calculated intensities from the structure model are used to carry out this convolution sum, it is found that with increasing fraction m the R factor can be lowered to, for example, 0.22 (as shown for two data sets). [Note that a more complete correction would involve multiple convolutions of $I_{\mathbf{h}}$, each with its own weight (Cowley, Rees & Spink, 1951).]

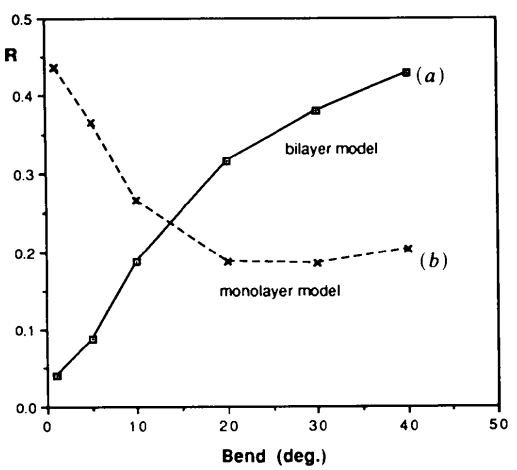

Fig. 5. Comparison of simulated electron diffraction intensities from a bend-deformed crystal to (*a*) the intensities from an undeformed unit cell and (*b*) the intensities from a single boric acid layer. The crystallographic R factor is calculated for 133 reflections. It is clear that, if the structure were significantly bend-deformed, the observed intensities should resemble those from a monolayer.

To summarize these studies, it is clear that microcrystals of boric acid diffract as if single layers were independent from one another. The cause for this must be due to a stacking disorder as discussed by Cowley (1953) in his original study. This is supported by the continuous reciprocal-lattice rods observed as one tilts single crystals and also by the applicability of a secondary scattering correction to the intensity data. Direct phasing invariably leads to only a single-layer structure where heavy-atom bond distances and angles agree well with X-ray and neutron diffraction determinations. Definition of H-atom positions, on the other hand, cannot be made with any precision, probably due to the secondary scattering perturbation.

This research was supported in part by a grant from the National Science Foundation (CHE9113899).

References

COWLEY, J. M. (1953*a*). *Acta Cryst.* **6**, 516-521.
COWLEY, J. M. (1953*b*). *Acta Cryst.* **6**, 522-529.
COWLEY, J. M. (1961). *Acta Cryst.* **14**, 920-927.
COWLEY, J. M. & GOSWAMI, A. (1961). *Acta Cryst.* **14**, 1071-1079.
COWLEY, J. M., REES, A. L. G. & SPINK, J. A. (1951). *Proc. Phys. Soc. London Sect. A*, **64**, 609-619.
CRAVEN, B. M. & SABINE, T. M. (1966). *Acta Cryst.* **20**, 214-219.
DORSET, D. L. (1989). *J. Electron Microsc. Tech.* **11**, 298-309.
DORSET, D. L. (1991*a*). *Acta Cryst.* **A47**, 510-515.
DORSET, D. L. (1991*b*). *Ultramicroscopy*, **38**, 23-40.
DORSET, D. L. & HAUPTMAN, H. A. (1976). *Ultramicroscopy*, **1**, 195-201.
DOYLE, P. A. & TURNER, P. S. (1968). *Acta Cryst.* **A24**, 390-397.
DVORYANKIN, V. F. & VAINSHTEIN, B. K. (1960). *Sov. Phys. Crystallogr.* **5**, 564-574.
GAJHEDE, M., LARSEN, S. & RETTRUP, S. (1986). *Acta Cryst.* **B42**, 545-552.
HAUPTMAN, H. A. (1972). *Crystal Structure Determination. The Role of the Cosine Semivariants.* New York: Plenum.
HAUPTMAN, H. (1975). *Acta Cryst.* **A31**, 680-687.
HAUPTMAN, H. & GREEN, E. A. (1976). *Acta Cryst.* **A32**, 45-49.
HAUPTMAN, H. & KARLE, J. (1953). *Solution of the Phase Problem I. The Centrosymmetric Crystal.* ACA Monogr. No. 3. Washington, DC: American Crystallographic Association.
KARLE, I. L., DRAGONETTE, K. S. & BRENNER, S. A. (1965). *Acta Cryst.* **19**, 713-716.
LOBACHEV, A. N. & VAINSHTEIN, B. K. (1961). *Sov. Phys. Crystallogr.* **6**, 313-317.
MOSS, B. & DORSET, D. L. (1982). *J. Polym. Sci. Polym. Phys. Ed.* **20**, 1789-1804.
VAINSHTEIN, B. K. (1955). *Zh. Fiz. Khim.* **29**, 327-344.
VAINSHTEIN, B. K. (1964). *Advances in Structure Research by Diffraction Methods*, edited by R. BRILL, Vol. 1, pp. 24-55. New York: Wiley Interscience.
WILSON, A. J. C. (1942). *Nature (London)*, **150**, 151-152.
ZACHARIASEN, W. H. (1934). *Z. Kristallogr.* **88**, 150-161.
ZACHARIASEN, W. H. (1954). *Acta Cryst.* **7**, 305-310.